Irrigation Sciences and Engineering (JISE) Vol. 43, No. 4, Winter 2021, Original Paper p. 33-49

Investigating the Effect of Different Arrangements of Obstacle on the Stepped Spillway on Flow Characteristics and Energy Dissipation

Seyed Amin Asghari Pari[1*] and Mojtaba Kordnaeij[2]

1*- Corresponding Author, Associated Professor, Civil Engineering. Engineering Faculty, Behbahan Khatam Alanbia University of Technology *(Asghari_amin@bkatu.ac.ir).*

2- Lecturer, Master of River Engineering, Civil Engineering. Engineering Faculty, Behbahan Khatam Alanbia University of Technology.

Received: 10 January 2021 Revised: 3 February 2021 Accepted: 6 February 2021

Abstract

This study has investigated the effect of roughness such as screen and 3D-porous obstacle with different arrangements on steps, 3D-porous obstacle, and continuous obstacle at the edge of steps in two slopes of 1:2 and 1:3 for all three regimes in the stepped spillways. The image processing results showed that the roughness of the spillways makes the recirculation zone under the pseudo-bottom smaller and a transparent region is formed in the inner corner of the spillway where there is no air bubble. Moreover, adding roughness on bottom and placing the 3D-porous obstacle and continuous obstacle on the edge of step in the step spillway cause the inception point of free aeration move down to the downstream compared with flat steps on both slopes. The placement of the 3D-porous obstacle and screen in all arrangements, as well as the continuous obstacle and 3D-porous obstacle on the edge of the spillway at 1:2 slope do not have a positive effect on the energy dissipation on transition and skimming flow regimes; however, by placing the obstacle at the edge of the spillway with a 1:3 slope, the dissipation performance of the spillway increased for all three regimes with an average of +5%.

Keywords: Stepped Spillway, Energy Dissipation, 3D-Porous Obstacle, BIV.
DOI: 10.22055/jise.2021.36213.1940.

Introduction

Stepped spillways are hydraulic structures considered by designers due to the relatively low cost, the fast manufacture, and the high energy dissipation. The flow's general behavior may be characterized by three different regimes, namely nappe, transitional, and skimming flow (Ohtsu, 1997 & Chanson., 2002). Nappe flow occurs at a low flow rate and can be defined as a succession of free-falling nappes. In the skimming flow, the water (or air-water) flows as a coherent stream over the pseudo-bottom formed by the step's outer edges; beneath it, a three-dimensional vortex occurs (Matos et al., 1999; Chanson, 2002; Gonzalez & Chanson, 2008) which helps dissipate energy (Carosi & Chanson, 2008). For the typical hydraulic design of stepped spillways, a skimming flow regime is appropriate (Chanson, 1995, 2002; Matos, 2000; Boes and Hager, 2003).

Extensive studies have been carried out by researchers on the understanding of flow in the stepped spillways. In the case of using obstacles with different shapes and roughness, Guenther et al. (2013) conducted a study on the effect of continuous, staggered, and one-sided obstacle; Aal Gemal et al. (2018) studied the effect of obstacle height at the edge of the spillway; Felder and Chanson (2014) investigated the edge with different porosities; Al-Husseini (2016) studied on roughening of the bottom with aggregate and making an inclined edge. In general, the results of the research indicate the positive dissipation effect of obstacle on the edge. Regarding the effect of shape and type of roughness on the bottom, a systematic research was conducted by Gonzalez et al.

(2005 & 2008) and Takahashi et al. (2006) who stated that the screen used in the bottom on their slope which was 1:2 moved the aeration point downstream compare with flat step. In this situation, the recirculation zone beneath the pseudo-bottom became smaller and energy dissipation decreased, which was undesirable. The results of Bung (2010) and Bung and Schlenkhoff (2010) about using pyramidal roughness on the bottom also indicated that the aeration point either did not change or was not transferred to the downstream of the spillway depending on the roughness arrangement. The gabion stepped chute which was used by Wüthrich and Chanson (2014) showed that the rate of energy dissipation on the gabion was lower than the flat steps.

The 3D-Porous Obstacle (the following is named 3DPO) was used as an energy dissipation structure by Kordnaeij et al. (2017) to control turbidity current which had a better dissipation effect than the porous plate (2D) under the same conditions due to the formation of the rotational area inside the 3DPO. Then, Saeidi et al. (2017), in their study of jump control using 3DPO, showed that this type of structure also had a positive effect in high-speed flows. Therefore, in the present research, the 3DPO function in energy dissipation in stepped spillway has been investigated.

It is possible to use the Particle Image Velocimetry (PIV) technique to measure the turbulence structure in different conditions to have access to some disturbance scales (Goepfert et al., 2004). On the other hand, PIV is subject to measurement limitations and cannot be used when the air flows into the air and the bubbles appear (Chang and Liu, 1998). Hence, by using the PIV technique, Amador et al (2004) investigated the non-aeration area of the stepped spillway that occurs in skimming flow regime in the initial steps (Amador et al., 2004). The use of Bubble Image Velocimetry (BIV) technique was first conducted by Ryu et al. (2005). Emadzadeh and Chiew (2017) investigated a hydraulic jump using PIV and BIV combinations for air-bubble-free and air bubbles areas. By combining the SIM, HSPIV, BTM, and BIV methods in a chute spillway, Yang et al. (2018) eventually understood the two-phase flow. The results of Leandro et al. (2014) about using BIV in stepped spillway showed that the difference between the results of image processing and probe up to 15% could be due to the fact that probe measures concentration and velocity of the bubble at the center of the flume, while by using the BIV technique, the measurement can be done next to the flume glass which may lead to different results. On the other hand, it was stated that measuring velocity using probe is not necessarily correct and errors might happen up to about 5%. Following the research conducted by Leandro et al., Bung and Valero (2015) used the BIV technique to measure the bubble's velocity on the step in aerated flow conditions. In Table (1), a summary of the researches conducted based on image processing is presented in stepped spillway in the aerated area. In this table, θ is the stepped spillway slope, W is the width of the flume, q is the quantity (discharge) unit width, and d_c/h is the dimensionless parameter in which h is the step height and d_c is the critical depth of the flow, which is obtained by the relation $d_c = (q^2/g)^{1/3}$.

In this research, two goals have been investigated. The first goal is to investigate the effect of creating a type of roughness with a specific geometry (3DPO) on the stepped spillway bottom and also on the edge of the spillway steps in two slopes and different flow regimes and its effect on the energy dissipation of the downstream. The second goal is better understanding of the flow regime passing through the 3DPO and Screen at the spillway bottom using the BIV technique.

Table 1- Summary of Experimental Studies of Air-Water Flow Properties on Step Spillway with an Image Processing Technique

Reference	*θ (°)*	*W (m)*	$q(m^2/s)$	d_c/h (-)	*Method*
Leandro et al (2014)	18.4;26.6	0.3	0.07 to 0.11	1.3 to 3.6	BIV
Bung and Valero (2015)	26.6	0.5	0.07	---	BIV
Bühler et al (2015)	26.6	0.3	0.09	---	IPP*
Bung and Valero (2016a)	26.6	0.3; 0.5	0.07	1.3	BIV/OF
Bung and Valero (2016b)	26.6	0.5	0.07	1.3	OF**
Lopes et al (2015)	26.6	0.5	0.07	1.3	BIV
Kramer and Chanson (2019)	45.0	0.985	0.067	0.8	OF
Kramer and Chanson (2018c)	48	0.99	0.067	0.8	VC***
Zhang and Chanson (2018)	45.0	0.985	0.083	0.9	OF
Current Study	19.2;27.5	1.2	0.122	1.06	BIV

*IPP: Image Processing Procedure, **OF: Optical Flow and ***VC: High-speed video Camera

Dimensional Analysis

The most important flow variables on the stepped spillways are the properties of the fluid and hydraulic of flow including critical depth of water (dc), velocity (V), geometry of the spillway including step height (h), step length (l), width of spillway (w), number of steps (N_0), acceleration of gravity (g), dynamic viscosity (μ), mass density (ρ), and arrangement of obstacle on step (Sh_o). The total head loss is expressed by $\Delta H = H_t - H_1$, where H_1 is the head on the considered step and H_t is the upstream head of the spillway. The function through which the relation of variables can be expressed is:

$$f(N_0, l, h, V, dc, W, g, \rho, \mu, Sh_o, H_t, H_1) = 0 \quad (1)$$

Using Buckingham's π theory one can obtain

$$= f\left(\frac{H_t - H_1}{H_1}, \frac{d_c}{h}, \frac{h}{l}, \frac{w}{l}, Re, Fr, \text{No}, Sho\right) \quad (2)$$

As in this study, the number of steps and the width of spillway are held constant; Reynolds number is between 3.45×10^4 and 1.05×10^5. Then it is assumed that the force of fluid viscosity is insignificant compared to the inertia force for open channel flow (Chow, 1959); so three dimensionless variables of Reynolds number Re ,N_o and $\frac{w}{l}$ could be eliminated. The equation (2) is presented below:

$$\frac{H_t - H_1}{H_1} = = f\left(\frac{d_c}{h}, \frac{h}{l}, Fr, Sho\right) \quad (3)$$

Materials and Methods

The flume used was direct, with a length of 10 m, a width of 1.2 m, and a height of 1.2 m in the first 2 m, and 1 m in length of the flume. The maximum flow rate of 150 liters per second discharged by two pumps, where an Ultrasonic Flow Meter installed on the pump's outlet was used to measure the quantity discharged. The flume walls were made of transparent glass and a metal bottom. The two spillways have eight steps, where the vertical length of step (h) is 10.9 cm, at the 1:3 slope, the horizontal length of step (L) is 31.3 cm, and the total height is 87 cm, while at a 1:2 slope, the length of step is 20.9 cm and the total height is 88 cm.

Measurement of water depth in the tail-water was carried out using a point gage with an accuracy of ± 1 mm in the area after the downstream spillway jump. Another point gage with the same specifications was used for the upstream of the spillway to measure dc.

In all conducted experiments, the flume end gate was adjusted in such a way to place the jump at the toe of the spillway. The difference in energy upstream and downstream of the spillway (toe) was used, where the desired depth was measured using point gauge, to calculate energy dissipation. The equation (4) shows the noted relation. In any of the experiments of the research, the jump was not submerged, and therefore, to calculate the initial depth of the jump, Belanger relation was used (1828).

$$\Delta H = H_t - H_1 = (1.5d_c + P) - \left[y_1 + \frac{V_1^2}{2g}\right] \quad (4)$$

Equation (5) was used to calculate the relative drop .

$$\frac{\Delta H}{H_t} = \frac{H_t - H_1}{H_t} = 1 - \frac{H_1}{H_t} = 1 - \frac{[y_1 + \frac{V_1^2}{2g}]}{(1.5d_c + P)} \quad (5)$$

In the above relations V_1 is the flow velocity in the spillway toe (m/s), $y_1$is the initial depth of flow after the spillway (m), P is the total spillway height (m), and ΔH is the energy drop (m).

The length of the inlet in both spillways is 58 cm (Kramer & Chanson, 2018a). The image was recorded by Sony FS5 camera with 240 frames per second, along with 3 LED150 projectors. To adjust the focal distance of the camera, a 20×20 cm mesh grid screen with a 2×2 cm screen was used. In all experiments, camera adjustment was set before turning on the pumps. Figure (1) shows the overview of the spillway situation, the location of the camera along with the rails and the status of the projectors (LED) in the flume.

In the present study, two screens with different height were used. The screen used has a thickness, length, and width of 0.3, 1.5,8 and 1.5 cm. The height of the screen was chosen as 1 cm and 2.1 cm, respectively. A screen with a height of 2.1 cm was selected for the same height as the obstacle. The 3DPO used has been cubic with the dimension of 2.1 cm and porosities in circles with a diameter of 0.9 cm and a volume porosity of approximately 25% (Figure. 2).

Table (2) and Figure (3) represent different patterns and arrangements of obstacles. For slope 1:2, 64 experiments and for slope 1:3, 40 experiments were carried out. In Table (2), Y stands for the tests performed and N shows the tests that were not performed.

Fig. 1- Flume, Spillway, LED, Rail, and Location of Camera (Slope 1:2, θ=27.5°)

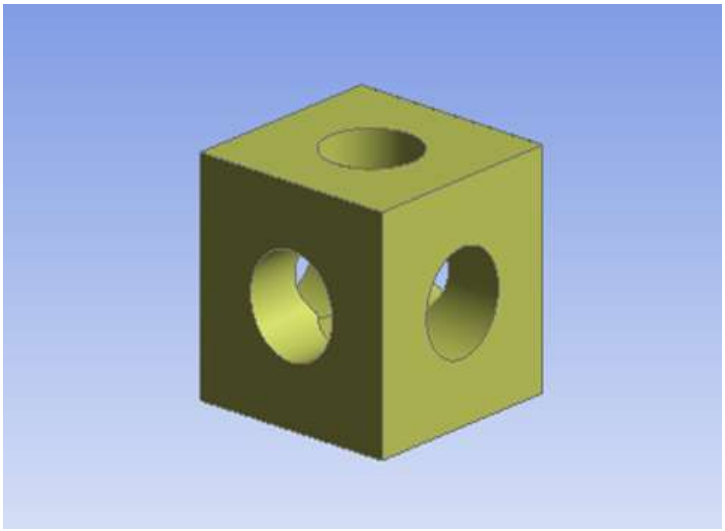

Fig. 2- 3DPO

Image processing model

Image processing was performed with a frame rate of 240 and in 8 s (Camcorder Limit) with the image dimensions of 1920 × 1080 pixels. The recalled images were used for each experiment in the PIVlab code (Thielicke & Stamhuis, 2014) with a 128 × 128-pixel resolution interrogation area and 75% overlapping with optimal filters based on the results of Bung and Valero (2015).

Table 2- Summary of Tests

θ°	dc/h	Flat Step	Screen 1 cm	Screen 2.1 cm	Fully covered with 3DPO	Edge continuous 3DPO	Zigzag 3DPO (Continuous)	Zigzag 3DPO with a gap	Edge continuous obstacle
19.2	0.46-10.6	Y	Y	N	Y	Y	N	N	Y
27.5	0.46-10.6	Y	Y	Y	Y	Y	Y	Y	Y

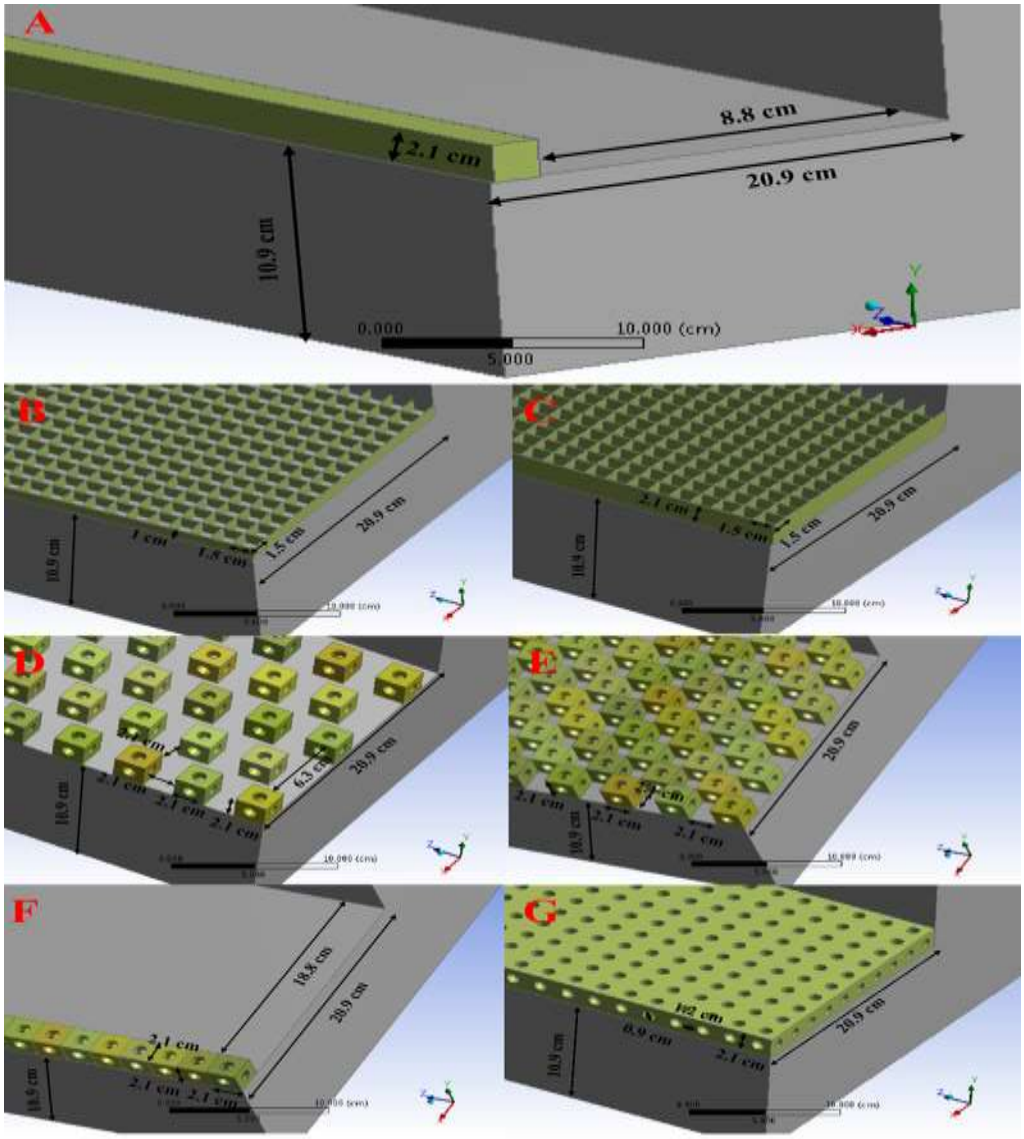

Fig. 3-Model type, Slope 1:2 (θ=27.5°), A: Edge Continues Obstacle, B: Screen 1 cm, C: Screen 2.1 cm, D: Staggered 3DPO with a gap, E: Continuous Staggered 3DPO, F: Edge continuous 3DPO and G: Fully covered with 3DPO.

Results and Discussion

Flow Properties

In the flat steps, the screen with different heights and the 3DPO with different arrangements in both slopes of 1:3 and 1:2, the surface flow patterns are different from the arrangements of continuous obstacle and continuous 3DPO edge of step. For this purpose, the water height was measured on the edge of step 6, and the results are presented in Table (2) for dc / h = 0.64 (transition flow representative) and dc / h = 1.06 (skimming flow representative). In Table (2), dw is the height of the water measured from the spillway bottom and perpendicular to it and dw/h is non-dimensional parameter of flow relative height. In the cases where (-) is presented, the experiment has not been conducted and this symbol is presented as the same in the following tables.

Based on Table (2) and observations, placing roughness (screen and 3DPO) on the bottom and an obstacle (continues wood and 3DPO) at the edge of steps in the transitional flow regime increase the surface oscillations of the flow, and hence, the relative height of the flow increases as compared to the flat step. This changes the flow regime from transition to skimming and affects all of the research tests, reduced surface fluctuations, and reduced relative height of flow. In the skimming flow regime, the relative height of the roughness flow on the bottom of steps varies with the edge obstacle relative to the flat step. The roughness at the bottom of the step causes the relative height of the flow to decrease relative to the flat step, but the obstacle at the edge of the step increases the flow's relative height.

If the spillway is designed for high discharge, the structure will operate correctly in the lower discharge and the designer must consider fluctuations for the transitional flow (Bung, 2013). Therefore, it is necessary to know the approximate water level surface to construct spillway side walls to prevent water from pouring to the surrounding area. All of the present arrangements by adding screen with different height and 3DPO on the bottom as well as obstacle and 3DPO in the edge of step showed that in the transitional flow regime, the relative height of the flow was much higher than skimming flow and has more fluctuations; this effect is more prominent when obstacle is placed on the edge of step.

Inception Point (IP) of free aeration

The results of starting the IP for various arrangements have been presented in Table (3). As the spillway slope increases from 1: 3 to 1: 2, the distance required for the development of the boundary layer increases so that the IP in identical flow discharge (dc/h = 1.06) has moved a step downstream and shifted from step 3 at 1:3 to step 4 at 1:2. Adding a screen with two different heights and a 3DPO with different arrangement on the step bottom showed that this roughness has caused the IP's prolongation as long as two steps compared to the flat step. But the placement of continuous obstacle and continuous 3DPO on the edge of steps has increased the IP as far as one step compared to the flat. During the test, visual observations indicate that the number of bubbles observed on the step bottom for screen with different height and 3DPO with the different arrangement was less than that of the flat step, continuous obstacle, and continuous 3DPO on the edge of steps.

Table 2- Summary of Water Height at Edge of Steps 6

Step 6	dw/h(dc/h=0.64)		dw/h(dc/h=1.06)	
	θ=27.5	θ=19.2	θ=27.5	θ=19.2
Flat Step	1.28	1.41	1	1.25
Screen 1 cm	1.57	1.53	0.83	1.16
Screen 2.1 cm	1.7	-	0.86	-
Fully Covered with 3DPO	1.72	1.73	0.83	1.20
Continuous Staggered 3DPO	1.40	-	0.91	-
Staggered 3DPO with a gap	1.35	-	0.8	-
Edge Continuous 3DPO	1.57	1.75	1.07	1.31
Edge Continuous Obstacle	1.86	2.06	1.28	1.44

 DOI: 10.22055/jise.2021.36213.1940

Table 3- Summary of Inception Point (IP)

dc/h=1.06	*Flat Step*	*Screen 1 cm*	*Screen 2.1 cm*	*Fully covered with 3DPO*	*Edge continuous 3DPO*	*Staggered 3DPO (Continuous)*	*Staggered 3DPO with a gap*	*Edge continuous obstacle*
θ=19.2	3	5	-	5	4	-	-	4
θ=27.5	4	6	6	6	5	6	6	5

The results of Gonzalez et al. (2005 & 2008) and Takahashi et al. (2006), Bung (2010), Bung and Schlankhov (2010), as well as the results of the present study on the placement of any obstacle including screening, solid pyramidal roughness, and 3DPO with different arrangements on the spillway bottom for skimming flow regime indicate that these obstacles generally cause prolongation of the development of the boundary layer and transition the IP to the downstream of the spillway compared to the flat step. On the other hand, due to the transition of the IP to the downstream, it can be expected that the placement of the 3DPO (different shape and arrangement) on the bottom will have a negative dissipation effect.

Flow Regime

Many laboratory studies have been conducted to determine the assessment criteria for starting the flow regimes based on relative critical depth (dc/h) and chute geometry (h/l). Most studies evaluate flow regimes using visual observations. Therefore, there is a wide dispersion of empirical criteria for the initiation of transitional and skimming flows (Ostad Mirza, 2016). The relationships presented for classifying the flow regime in a stepped spillway, such as Chanson (1995-2001) and Chanson et al. (2015), are used to distinguish the nappe, transition, and skimming in the flat stepped spillway. Creating screen and 3DPO in different arrangements on the bottom and edges of steps may change the flow regime.

For continuous obstacle on the step edge, studies by Kökpinar (2004) showed that the obstacle on the edge of step causes the flow regime onset changes compared to the flat steps. Therefore, in the following section, it has been tried to determine the boundary of different flow regimes according to the observations made during the test; films and photos recorded. In this classification, the nappe flow has been considered for stepped nappe states without the air bubble rotation. The transitional flow refers to a case where there is an air pocket in the step and the recirculation flow has been formed on the pseudo-bottom, the skimming flow refers to when there is no air pocket in the step and recirculation flow is formed in the bottom. In Table (4), the flow regime classification has been given in which NAP, TRA, and SKI represent the nappe flow, the transitional flow, and the skimming flow, respectively

Regarding the flow regime results, it can be seen that the placement of screen and 3DPO with different arrangements on the bottom and the edge of step cause onset of the transitional and skimming flow regime occurs in lower dc/h compare to flat step. In contrast, the result of Gonzalez et al. (2008) showed that the step roughness had no influence on the type of flow regime. This difference in the flow regime's onset is due to the higher roughness height used in the present study (1 cm and 2.1cm) compared to that used in Gonzalez et al.'s study (0.8cm). Therefore, it can be stated that the relative roughness height greater than 0.092 (roughness height to step height) can change the flow regime.

Table 4- Flow Observation for Various Step Pattern

dc/h	θ	Flat step	Screen 1 cm	Screen 2.1 cm	Fully covered with 3DPO	Staggered 3DPO (Continuous)	Staggered 3DPO with a gap	Edge Continuous 3DPO	Edge Continuous obstacle
0.46	19.2	NAP	NAP	-	NAP	-	-	NAP	NAP
0.55	19.2	NAP	NAP	-	NAP	-	-	NAP	TRA
0.64	19.2	NAP	TRA	-	TRA	-	-	TRA	TRA
0.73	19.2	TRA	TR-SK	-	TRA	-	-	TRA	TRA
0.83	19.2	TRA	SKI	-	SKI	-	-	SKI	SKI
0.92	19.2	TRA	SKI	-	SKI	-	-	SKI	SKI
1.01	19.2	SKI	SKI	-	SKI	-	-	SKI	SKI
1.06	19.2	SKI	SKI	-	SKI	-	-	SKI	SKI
0.46	27.5	NAP	NAP	NAP	NAP	NAP	NAP	NAP	NAP
0.55	27.5	NAP	TRA	TRA	TRA	TRA	TRA	TRA	TRA
0.64	27.5	TRA	TRA	TRA	TR-SK	TRA	TRA	TR-SK	TRA
0.73	27.5	TRA	SKI	SKI	SKI	SKI	SKI	SKI	SKI
0.83	27.5	SKI	SKI	SKI	SKI	SKI	SKI	SKI	SKI
0.92	27.5	SKI	SKI	SKI	SKI	SKI	SKI	SKI	SKI
1.01	27.5	SKI	SKI	SKI	SKI	SKI	SKI	SKI	SKI
1.06	27.5	SKI	SKI	SKI	SKI	SKI	SKI	SKI	SKI

Investigating of Streamlines on the Steps by Using the Results of BIV:

Figures (4) and (5) show BIV result in both slopes 1:2 and 1:3. Under the pseudo - bottom, for flat step (5A and 6A), there are two main areas on each of the steps on skimming flow regime. The first region, in which the flow is circulating, is called the recirculation zone (RZ), and the second region, where the flow (part of the flow or the entire flow after the RZ) collides with the bottom of the step, is called the mixing zone (MZ). These areas are consistent with the results of Zare and Doering (2012 a & b) and Lopes et al. (2017).

By adding a screen to the step bottom, similar to the results of Gonzalez et al. (2008) and Takahashi et al. (2006), a clear, non-bubble zone (CZ) was formed in the inner corner of step that were located after the IP to the downstream. In the bottom of steps, the 3DPO with different arrangements similar to the screen, the flow of the CZ was formed in the inner corner of the steps. Placing roughness on the steps with different shapes (Screen and 3DPO) and different arrangements (continuous and staggered) cause the clockwise RZ of the step to start from the boundary of the MZ on the step, and to collide with the floor roughness. The result is a reduction of the RZ amplitude at the bottom of the step. Reducing the RZ amplitude causes the bubbles to reach the step's inner corner, thus forming a transparent water area without bubbles. On the other hand, due to the roughness of the bottom and the decrease of the recirculating height, the RZ is transformed from circular to elliptical. (Figure. 4B & C, Figure. 5C to F).

 DOI: 10.22055/jise.2021.36213.1940

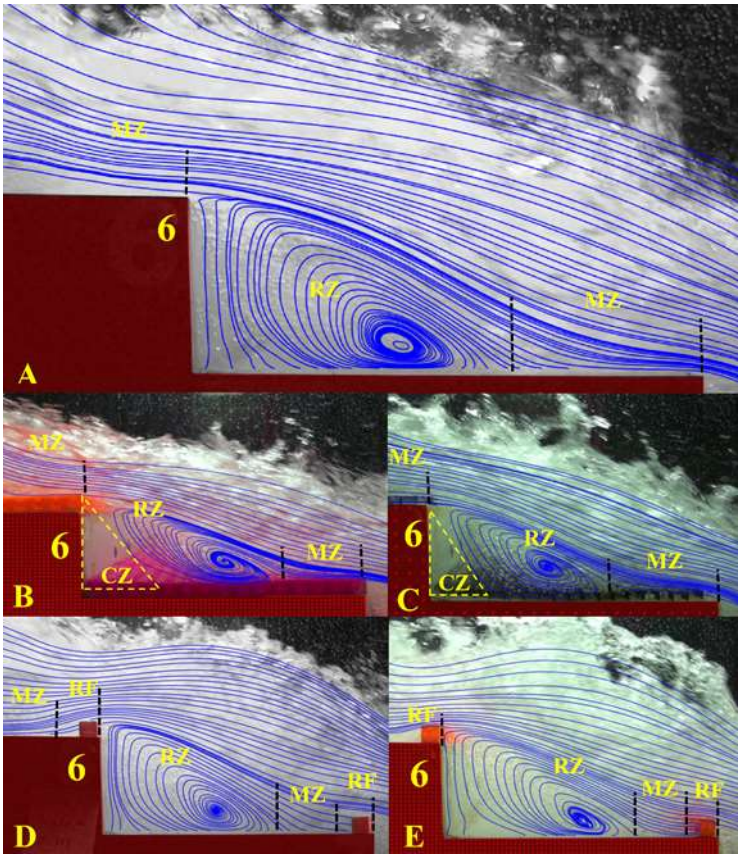

Fig. 5- Streamline on step, dc/h=1.06, Slope 1:3 (θ=19.2°), A: Flat step, B: Fully covered with 3DPO, C: Screen 1cm, D: Edge continuous obstacle and E: Edge continues 3DPO.

Placing the porous and continuous obstacles at the edge for both slopes, the RZ and MZ have become similar to the flat step and CZ is removed. Placing an obstacle on the edge of the steps create new zones. The continuous obstacle, beyond the MZ flow interaction with obstacle on the edge of steps, is redirected towards the main flow which is called Redirected Flow (RF) (D & E in Figures 4 and G & H in Figures 5). Also, in the case of edge obstacle at slope 1:2, it was not possible to distinguish the RF and RZ regions on the pseudo bottom. Therefore, the area was named RZ-RF (Figures 5 H).

In the case that the screen is located on the step bottom, the motion of the bubbles within the screen due to the closure of the screen only has fluctuating state, while the bubbles inserted inside the porous have circulated due to the internal porosity spherical geometry.

Investigation of the Flow Velocity Profile at the Edge of the Steps Spillway

The results of Bung and Valero (2015) showed that the velocity obtained from BIV is less than that obtained from the CP (Conducted Probe), and the shape of the velocity profiles obtained from two methods is the same. Therefore, in this section, the velocity profile resulted from BIV at the edge of step 7 on different slopes and arrangement for dc / h = 1.06, which is the maximum discharge-all the flows formed in skimming flow regime have been presented.

The non-dimensional velocity profiles for different arrangements of this research on step 7 for skimming flow regime are shown in Figures (6) and (7). Regarding the Figure (6) on slope 1:2, putting the screen and 3DPO with the different arrangement on the spillway bottom causes that the maximum velocity increases relative to a flat step. It seems that the rough step (screen and 3DPO with different arrangement), affected flow separation at each step edge and shear layer development downstream of each step. This effect would induce drag reduction on rough step and increasing velocity of passing flow. Also, this effects on the rough step (screen with 8 mm height) spillway was reported by

Gonzalez et al. (2005 & 2008) and Takahashi et al. (2006) on slope 1:2.

At 1: 3 slope (Figure 6), the velocity profile shows two zones of the maximum velocity at altitude, but this effect was not observed at 1: 2 slope (Figure 5). This effect appears to be due to the higher MZ and the possibility of collision and crossing the step at a 1: 3 slope compared to the 1: 2 slope as well as the mainstream crossing the step bottom. This effect was reduced when 3DPOs were positioned on the bottom and step edges due to passing through the 3DPOs.

The placement of a continuous obstacle on edge causes its velocity to reach zero to its equivalent height (2.1 cm), but at the location of 3DPO on the edge, the velocity is not zero due to flowing through the porosity. Comparison of flat step velocity profiles on both slopes with continuous obstacle and continuous 3DPO states on the edge indicates that the lower velocity in this case compared with the flat one.

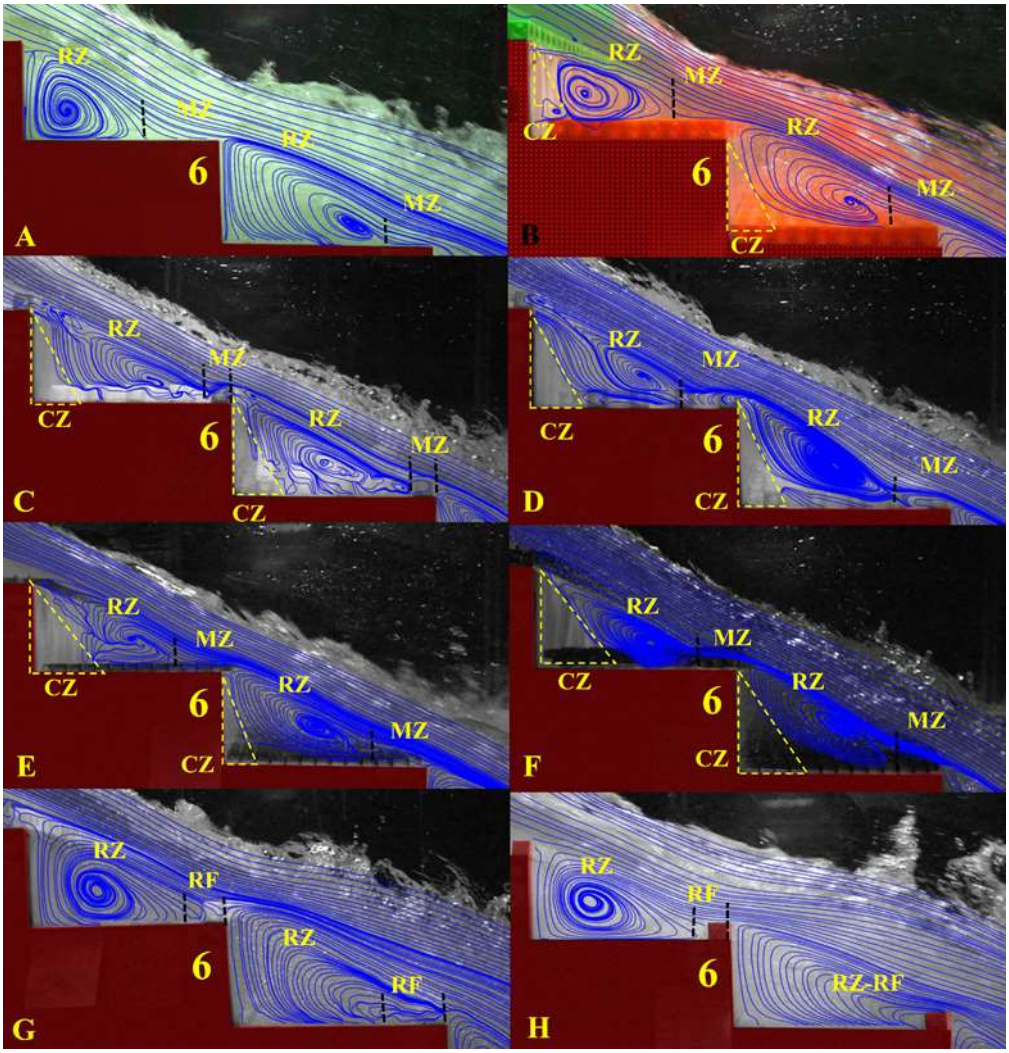

Fig. 6- Streamline in pseudo bottom, dc/h=1.06, Slope 1:2 (θ=27.5°), A: Flat Step, B: Fully covered with 3DPO, C: Staggered 3DPO (continuous), D: Staggered 3DPO with a gap, E: Screen 1cm, F: Screen 2.1 cm, G: Edge continues 3DPO and H: Edge continuous obstacle.

 DOI: 10.22055/jise.2021.36213.1940

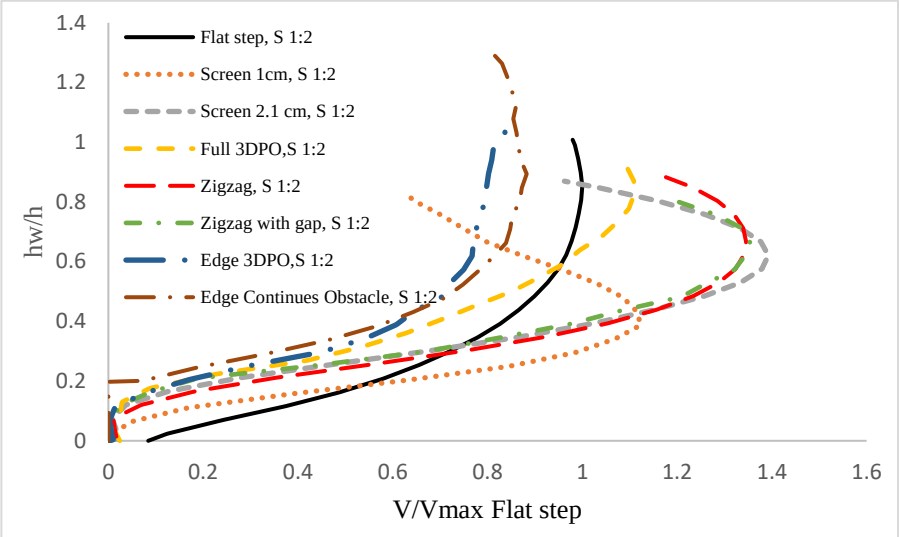

Fig. 7- Comparison of Velocity Profile on the Edge of Step 7, dc/h=1.06, Slope 1:2.

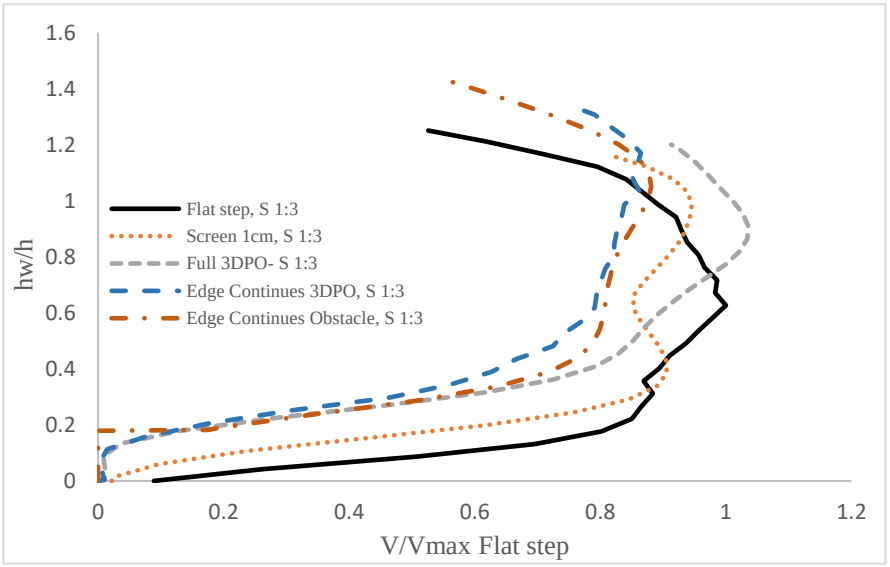

Fig. 8- Comparison of Velocity Profile on the Edge of Step 7, dc/h=1.06, Slope 1:3.

Effect of Energy Dissipation

The results of energy dissipation (Table 5 and Figures (9) and (10) show that in a flat step, the energy dissipation decreases by increasing the slope from 1: 3 to 1: 2 and this difference in the upper boundary of the transition regime and skimming flow is more obvious.

By increasing the discharge rate and changing the flow regime from the nappe flow to the transition and skimming flow regime, the difference in the different arrangement of the edges and the spillway bottom in the energy dissipation is shown to the nappe state, and this effect is less in 1:2 slope (Figure 9), which indicates that the 1: 3 slope is an effective obstacle in energy dissipation. For example, the rate of energy dissipation at (dc / h = 0.46) at slope of 1: 3 is equal to 86.37% and this amount at slope of 1: 2 is equal to 87.98%. With increasing the discharge, this difference increases so that in (dc / h = 1.06) in 1: 3 slope, the energy dissipation rate reaches 46.09% and for 1: 2 slope, the energy dissipation rate is 36.27%, which is the difference from 2% in the nappe flow regime to 10% in the skimming flow regime has arrived.

At 1:2 slope and dc/h = 0.46 (nappe flow regime), the effect of creating 3DPO on the bottom with different arrangements and screen with different heights in energy dissipation have been equal or more than the flat step (Staggered shifted increase to

89.95%). In these states, energy dissipation is affected by roughness and for staggered and staggered with gap arrangement affect is more significant. The input flow into the 3DPO with a distance has led to the recirculating flow formation inside it and this effect causes more energy dissipation. In fully 3DPO covered arrangement at nappe flow, the energy dissipation was reduced due to the roughness's reduced effective surface area compared with the staggered model (both arrangements). Putting Screen and fully 3DPO covered arrangement at a 1: 3 slope had a positive effect on increasing energy dissipation in the nappe flow regime similar to a 1: 2 slope.

In the skimming flow regime, the analysis of the BIV showed that at 1: 3 slope, the flow lines that pass through the edge of the steps are close to the horizontal state due to the larger length of the MZ, while at 1: 2 slope, the small length of the MZ has caused the flow lines to be inclines to the horizon.
The horizontal flow of the MZ at the 1: 3 slope increase the energy dissipation due to effective collision with the edge obstacle compared with the 1: 2 slope. It also appears that the impact of horizontal flow on the 3DPO due to the possibility of a rotational flow inside the 3DPO cavity causes more energy dissipation than the continuous obstacle to occur. In the same line of research, the effect of flow collision with the obstacle was investigated by Saeidi et al. (2017) in which the effect of 3DPO on increasing energy dissipation at the downstream of the ogee spillway, was compared to non-porous obstacles, and it was shown that 3DPO had better performance in energy dissipation.

The results of energy dissipation indicate that screen performance in two heights and 3DPO in different arrangements on the bottom do not have a positive dissipation effect on the transition and skimming regime in two slopes of this research.

Table 5- Summery of Energy Dissipation

dc/h	θ	Free	Screen 1 cm	Screen 2.1 cm	Full Porous	Staggered	Staggered Shifted	Edge Porous	Edge Wood
0.46	19.2	84.63	83.43	No	79.14	No	No	88.36	86.37
0.55	19.2	79.41	78.52	No	71.56	No	No	82.56	79.41
0.64	19.2	72.61	71.58	No	64.48	No	No	79.13	70.51
0.73	19.2	66.10	66.64	No	56.73	No	No	70.22	66.10
0.83	19.2	57.74	58.34	No	51.17	No	No	62.35	57.74
0.92	19.2	52.37	52.37	No	45.76	No	No	55.95	52.37
1.01	19.2	47.12	46.49	No	45.21	No	No	51.32	47.74
1.06	19.2	46.09	44.85	No	42.30	No	No	51.86	45.47
0.46	27.5	87.98	86.55	88.72	87.15	89.38	89.95	89.38	87.44
0.55	27.5	81.86	77.83	80.87	81.26	81.65	81.65	78.30	78.75
0.64	27.5	69.56	63.44	64.11	67.90	68.50	69.08	67.90	66.69
0.73	27.5	65.89	60.99	57.69	62.24	64.04	60.99	62.85	61.62
0.83	27.5	57.34	52.09	52.09	53.45	53.45	52.09	56.06	57.32
0.92	27.5	51.36	45.23	43.06	49.33	50.63	46.63	51.27	49.33
1.01	27.5	45.86	34.78	39.21	39.92	40.62	37.77	42.01	42.01
1.06	27.5	36.03	25.78	31.82	29.34	34.07	31.06	38.37	38.37

 DOI: 10.22055/jise.2021.36213.1940

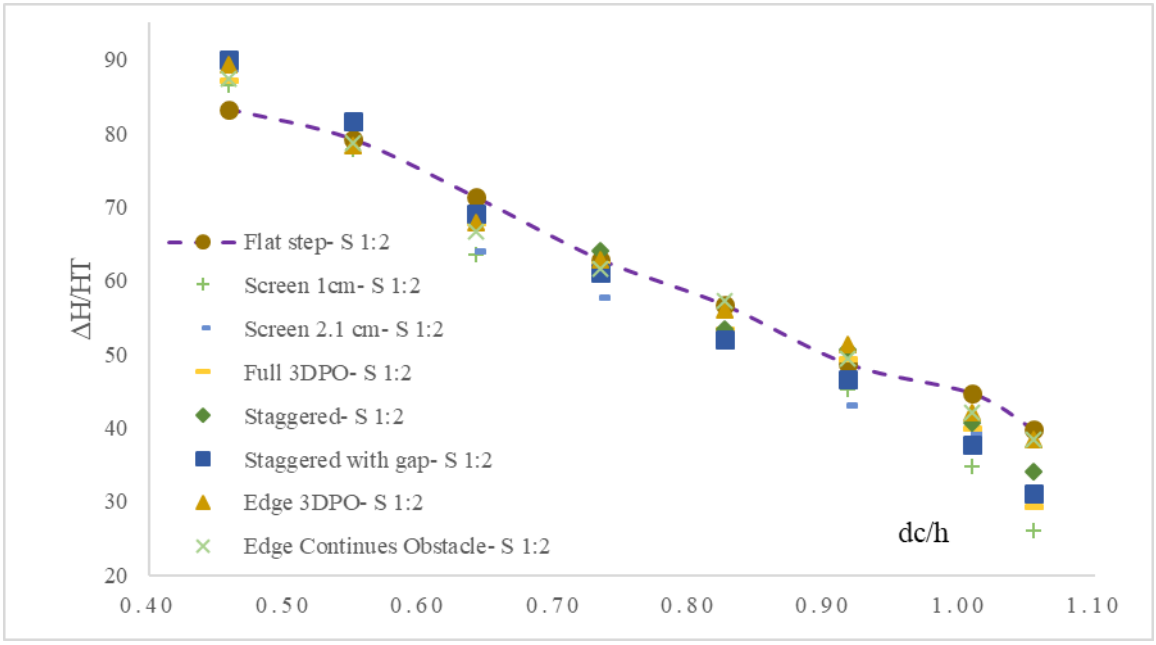

Fig. 9- Comparison of Energy Dissipation of Slope 1:2.

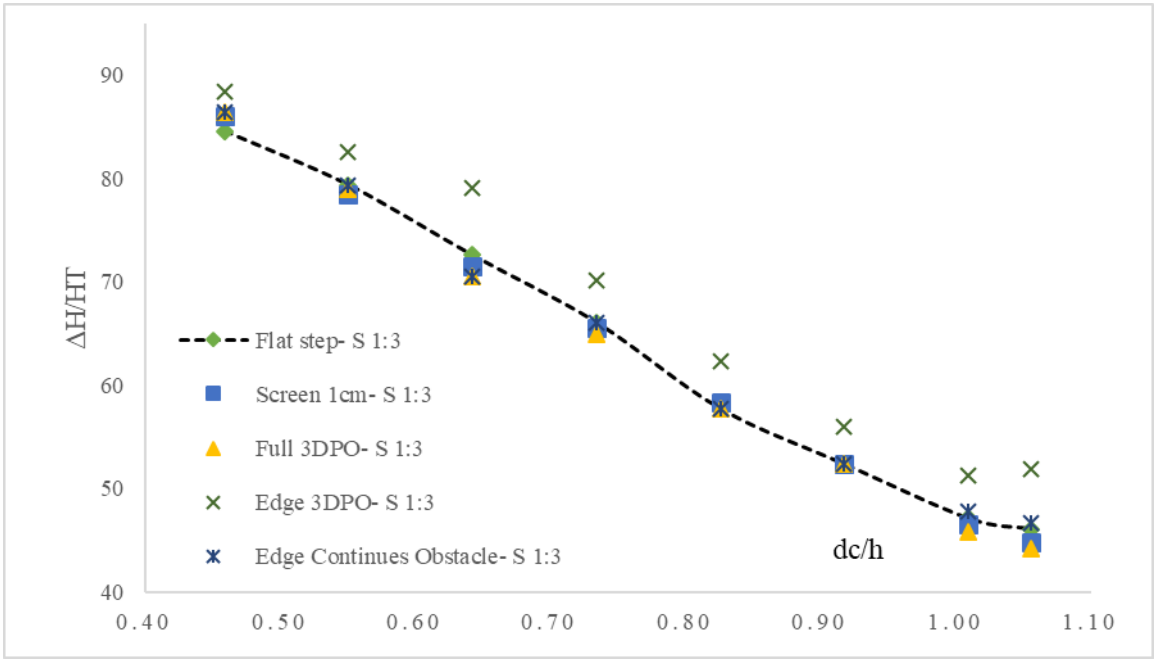

Fig. 10- Comparison of Energy Dissipation of Slope 1:3.

In general, it can be stated that the effect of roughness of different shapes and arrangements on the step spillway can be dependent on the flow regime in energy dissipation. For example, in the 1: 2 slope, for nappe flow regime, the screen and fully covered 3DPO arrangements have 1 to 4% less energy dissipation than the flat step, while other arrangements increased energy dissipation by up to 5% compared to the flat step. This mode is also set for the 1: 3 slope.

The results of Torabi et al. (2018), Wüthrich and Chanson (2014) for rough bed and gabion step spillway for the nappe flow regime showed that the roughness can increase the energy dissipation over the flat step. However, in the skimming flow regime, the gabion, the roughness and screening used by Wüthrich and Chanson (2014), Bung (2010), and Gonzalez et al. (2008) showed that these have no positive effect on energy dissipation. Therefore, according to the

results of the mentioned researchers and the results obtained from the present study, it can be concluded that the roughness of the step spillway with different arrangement in the nappe flow regime can increase energy dissipation and in transitional and skimming flow regimes have no positive effect on increasing energy dissipation compared to flat step.

On the other hand, according to the results of this study, the only obstacle in the skimming flow regime which can contribute to increased energy dissipation is either in the MZ or exposed to the main flow. The extent to which the obstacle in the MZ is effective in increasing energy dissipation, in addition to the obstacle location (Zare & Doering 2012), also depends on the type of obstacle and the stepped spillway slope (MZ length).

Conclusion

The present study compares the use of screen with two heights and 3 dimensional porous obstacle (3DPO) in the stepped spillway bottom with continuous, staggered, and staggered with distance arrangements and placement of continuous 3DPO and continuous obstacle at the edge of the step at two slopes of 1: 3 and 1: 2 in all three flows regime of nappe, transitional, and skimming. The image processing technique (BIV) has been used to better understand the flow properties.

1- The placement of screen and 3DPO with different arrangement on the spillway bottom causes that the start of the inception point of free aeration (IP) to be postponed, and hence, the IP is formed in a lower step (2 steps) than the flat step. However, the IP for the continuous obstacle and the 3DPO at the edge step, was transmitted to a lower step toward the downstream relative to flat step on both slopes of the present research.

2- The placement of screen and 3DPO with different arrangements on the bottom and the spillway edge cause that the flow regime boundary changes relative to flat step and direct the flow to the skimming regime at lower flow rates.

3- Placing roughness (screen and 3DPO) on the bottom of steps increases the flow velocity relative to the flat step, while the roughness (3DPO and continues) at the edge of steps reduces the flow velocity under the same slope and discharge conditions. As the flow velocity increases, the flow height decreases and the turbulence intensity level decreases.

4- The image processing results showed that in the case of a flat step, the vortices formed on the pseudo-bottom are formed adjacent to the vertical section of the step and, by increasing the slope from 1: 3 to 1: 2, the length of the mixing zone (MZ) decreases at the edge of the step. The size and shape of the recirculation zone (RZ) formed under the pseudo-bottom for the 3DPO arrangement and continuous obstacle at the spillway edge are similar to the flat step. The placement of screen and 3DPO with different arrangements on two slopes of 1: 2 and 1: 3 in skimming conditions showed that the clear water (CZ) without air bubbles form in the inner corner of the aerated step, which causes the dimension of the RZ to decrease relative to flat steps.

5- Energy dissipation in screen and various arrangements of 3DPO on the bottom in the transition and skimming flow regimes is less than flat step (for flat step at 1:2, it was average 5% more than other arrangements in skimming flow regime), but in a nappe regime, creating a roughness on the bottom, especially the a 3DPO, has increased energy dissipation. Creating a continuous obstacle and a continuous 3DPO at the edge of the step in 1: 3 slope, in which the length of the step was sufficient to create a MZ as well as an angle of flow of collision with an obstacle, has been effective in energy dissipation in all three flow regimes. But at 1:2 slope, where the MZ is very small, the continuous obstacle and continuous 3DPO have no effect on energy dissipation. Base on result of this study, it can be concluded in general that the arrangement and shape of roughness on the stepped spillway bottom in the transition and skimming regimes do not have a positive effect on the flow of energy dissipation, and obstacles can cause energy dissipation to be placed at the edge of the spillway (in MZ) and against the mainstream flow.

Acknowledgment

The authors are grateful for funding this project by Behbahan Khatam Alanbia University of Technology (BKATU).

References

1- Aal, G.M.A., Sobeah, M., Helal, E. and El-Fooly, M., 2018. Improving energy dissipation on stepped spillways using breakers. *Ain Shams Engineering Journal*, *9*(4), pp.1887-1896.

2- Amador, A., Van der Graaf, G., Sánchez-Juny, M., Dolz, J., Sánchez-Tembleque, F., Puertas, J. and Girona, C.J., 2004, July. Characterization of the flow field in a stepped spillway by PIV. In *Proc. 12th Symp. Applications Laser to Fluid Mechanics* (pp. 12-15).

3- Al-Husseini, T.R., 2016. A Novel experimental work and study on flow and energy dissipation over stepped spillways. *Journal of Babylon University-Engineering Sciences*, *24*(4).1050-1063.

4- Belanger, J.B., 1828. *Essai sur la solution numerique de quelques problemes relatifs au mouvement permanent des eaux courantes; par m. J.-B. Belanger*. chez Carilian-Goeury, libraire, des corps royaux des ponts et chaussees et des mines.

5- Boes, R.M. and Hager, W.H., 2003. Hydraulic design of stepped spillways. *Journal of Hydraulic Engineering*, *129*(9), pp.671-679.

6- Bühler, P., Leandro, J., Bung, D., Lopes, P. and Carvalho, R., 2015. Measuring void fraction of a stepped spillway with non-intrusive methods using different image resolutions. *IWHS 2015*, p.41.

7- Bung, D.B., 2010. A comparative study of self-aerated stepped spillway and smooth invert chute flow: The effect of step-induced macro-roughness. In *Chinese-German joint symposium on hydraulic and ocean engineering (CG JOINT 2010)* (pp. 451-456).

8- Bung, D. and Schlenkhoff, A., 2010. Self-aerated skimming flow on embankment stepped spillways: the effect of additional micro-roughness on energy dissipation and oxygen transfer.

9- Bung, D.B., 2013. Non-intrusive detection of air–water surface roughness in self-aerated chute flows. *Journal of Hydraulic Research*, *51*(3), pp.322-329.

10- Bung, D.B. and Valero, D., 2015, June. Image processing for bubble image velocimetry in self-aerated flows. In *36th IAHR World Congress* (pp. 6594-6601).

11- Bung, D.B. and Valero, D., 2016a. Optical flow estimation in aerated flows. *Journal of Hydraulic Research*, *54*(5), pp.575-580.

12- Bung, D.B. and Valero, D., 2016b, July. Image processing techniques for velocity estimation in highly aerated flows: bubble image velocimetry vs. optical flow. In *Proc. 4th IAHR Europe Congress* (pp. 151-157).

13- Carosi, G. and Chanson, H., 2008. Turbulence characteristics in skimming flows on stepped spillways. *Canadian Journal of Civil Engineering*, *35*(9), pp.865-880.

14- Chang, K.A. and Liu, P.L.F., 1998. Velocity, acceleration and vorticity under a breaking wave. *Physics of Fluids*, *10*(1), pp.327-329.

15- Chanson, H., 1995. Hydraulic design of stepped cascades, channels, weirs and spillways.

16- Chanson, H., 2001. Hydraulic design of stepped spillways and downstream energy dissipators. *Dam Engineering*, *11*(4), pp.205-242.

17- Chanson, H., 2002. *Hydraulics of stepped chutes and spillways*. CRC Press.

18- Chanson, H., Bung, D. and Matos, J., 2015. Stepped spillways and cascades. *Energy Dissipation in Hydraulic Structures." IAHR Monograph, CRC Press, Taylor & Francis Group, Leiden, The Nettherlands, H. Chanson Editor*, pp.45-64.

19- Chow, V. T. 1959. Open Channel Hydraulics. McGraw-Hill, New York, USA. Christodoulou, G. C. 1993. Energy dissipation on stepped spillways. *Journal of Hydraulic Engineering, Vol. 119, No. 5, pp. 644-650.*

20- Emadzadeh, A., Chiew, Y. M. 2017. Bubble Dynamics and PIV Measurements in a Hydraulic Jump. *The 37th IAHR World Congress August 13 – 18, Kuala Lumpur, Malaysia.*

21- Felder, S., 2013. Air-water flow properties on stepped spillways for embankment dams: Aeration, energy dissipation and turbulence on uniform, non-uniform and pooled stepped chutes.

22- Felder, S. and Chanson, H., 2014. Effects of step pool porosity upon flow aeration and energy dissipation on pooled stepped spillways. *Journal of Hydraulic Engineering*, *140*(4), p.04014002.

23- Goepfert, C., Marié, J. L. and Lance, M. 2004. Characterizing of an experimental device generating homogeneous and Isotropic turbulence by synthetic jets. The 9 th French Congress of Laser Velocimetry. ULB. Sept.14-17. Brussels. Belgium.

24- Gonzalez, C.A., Takahashi, M. and Chanson, H., 2005. Effects of step roughness in skimming flows: an experimental study.

25- Gonzalez, C.A., Takahashi, M. and Chanson, H., 2008. An experimental study of effects of step roughness in skimming flows on stepped chutes. *Journal of Hydraulic Research*, *46*(sup1), pp.24-35.

26- Gonzalez, C.A. and Chanson, H., 2008. Turbulence and cavity recirculation in air–water skimming flows. *Journal of Hydraulic Research*, *46*(1), pp.65-72.

27- Guenther, P., Felder, S. and Chanson, H., 2013. Flow aeration, cavity processes and energy dissipation on flat and pooled stepped spillways for embankments. *Environmental fluid mechanics*, *13*(5), pp.503-525.

28- Kordnaeij, M., Asghari Pari, S.A., Sajjadi, S.M. and Shafai Bajestan, M., 2017. Experimentally Comparisons of the Effect of Porous Sheets and Porous Obstacles in Controlling Turbidity Current. *Water and Soil Science*, *27*(1), pp.43-54.(In Persian)

29- Kökpinar, M.A., 2004. Flow over a stepped chute with and without macro-roughness elements. *Canadian Journal of Civil Engineering*, *31*(5), pp.880-891.

30- Kramer, M. and Chanson, H., 2018a. Transition flow regime on stepped spillways: air–water flow characteristics and step-cavity fluctuations. *Environmental Fluid Mechanics*, *18*(4), pp.947-965.

31- Kramer, M. and Chanson, H., 2019. Optical flow estimations in aerated spillway flows: Filtering and discussion on sampling parameters. *Experimental Thermal and Fluid Science*, *103*, pp.318-328.

32- Kramer, M. and Chanson, H., 2018. Free-surface instabilities in high-velocity air-water flows down stepped chutes.

33- Leandro, J., Bung, D.B. and Carvalho, R., 2014. Measuring void fraction and velocity fields of a stepped spillway for skimming flow using non-intrusive methods. *Experiments in Fluids*, *55*(5), pp.1-17.

34- Lopes, P., Bung, D.B., Leandro, J. and Carvalho, R.F., 2015, June. The effect of cross-waves in physical stepped spillway models. In *E-proceedings of the 36th IAHR World Congress. The Hague, the Netherlands* (Vol. 28).

35- Lopes, P., Leandro, J., Carvalho, R.F. and Bung, D.B., 2017. Alternating skimming flow over a stepped spillway. *Environmental Fluid Mechanics*, *17*(2), pp.303-322.

36- Matos, J., 2000, March. Hydraulic design of stepped spillways over RCC dams. In *Intl Workshop on Hydraulics of Stepped Spillways* (pp. 187-194). Balkema Publ.

37- Matos, J., Sanchez, M.A.R.T.Í., Quintela, A. and Dolz, J., 1999, August. Characteristic depth and pressure profiles in skimming flow over stepped spillways. In *Proceedings of the 29th IAHR congress, Graz, Austria*.

38- Ohtsu, I., 1997. Characteristics of flow condition on stepped channels. *The 27th Cong. of IAHR, Water Resources Engineering, Div./ASCE. San Francisco, USA, 1997*.Ostad Mirza, M. J. (2016). *Experimental study on the influence of abrupt slope changes on flow characteristics over stepped spillways* (No. THESIS). EPFL.

39- Ryu, Y., Chang, K.A. and Lim, H.J., 2005. Use of bubble image velocimetry for measurement of plunging wave impinging on structure and associated greenwater. *Measurement Science and Technology*, *16*(10), p.1945.

40- Saeidi, S., Asghari Pari, S., Shafai Bajestan, M. 2017 August. Laboratory study of the effect of porous roughness on hydraulic jump in a Stilling basin. *The Sixth national Conference of Architecture, Construction and Urban Environment.* (In Persian).

41- Takahashi, M., Gonzalez, C.A. and Chanson, H., 2006. Self-aeration and turbulence in a stepped channel: Influence of cavity surface roughness. *International journal of multiphase flow*, *32*(12), pp.1370-1385.

42- Torabi, H., Parsaie, A., Yonesi, H. and Mozafari, E., 2018. Energy dissipation on rough stepped spillways. *Iranian Journal of Science and Technology, Transactions of Civil Engineering*, *42*(3), pp.325-330.

43- Thielicke, W. and Stamhuis, E., 2014. PIVlab–towards user-friendly, affordable and accurate digital particle image velocimetry in MATLAB. *Journal of open research software*, *2*(1).

44- Valero, D. and Bung, D.B., 2015, June. Hybrid investigations of air transport processes in moderately sloped stepped spillway flows. In *E-proceedings of the 36th IAHR World Congress* (Vol. 28, pp. 1-10).

45- Wüthrich, D. and Chanson, H., 2014. Hydraulics, air entrainment, and energy dissipation on a Gabion stepped weir. *Journal of Hydraulic Engineering*, *140*(9), p.04014046.

46- Yang, J., Lin, C., Kao, M.J., Teng, P. and Raikar, R.V., 2018. Application of SIM, HSPIV, BTM, and BIV Techniques for Evaluations of a Two-Phase Air–Water Chute Aerator Flow. *Water*, *10*(11), p.1590.

47- Zare, H.K. and Doering, J.C., 2012. Effect of rounding edges of stepped spillways on the flow characteristics. *Canadian Journal of Civil Engineering*, *39*(2), pp.140-153.

48- Zare, H.K. and Doering, J.C., 2012. Energy dissipation and flow characteristics of baffles and sills on stepped spillways. *Journal of hydraulic research*, *50*(2), pp.192-199.

49- Zhang, G. and Chanson, H., 2018. Application of local optical flow methods to high-velocity free-surface flows: Validation and application to stepped chutes. *Experimental Thermal and Fluid Science*, *90*, pp.186-199.